analytical chemistry

ARTICLE

pubs.acs.org/ac

Thin Gold Film-Assisted Fluorescence Spectroscopy for Biomolecule Sensing

Amit Vaish,[†,⊥] Wei-Ssu Liao,[†] Mitchell J. Shuster,[⊗] Jennifer M. Hinds,[⊥] Paul S. Weiss,[*,†,‡,§,⊗,○] and Anne M. Andrews[*,†,∥,#]

[†]California NanoSystems Institute, [‡]Departments of Chemistry & Biochemistry and [§]Materials Science & Engineering, and [∥]Semel Institute for Neuroscience & Human Behavior, University of California, Los Angeles, Los Angeles, California 90095, United States

[⊥]Departments of Bioengineering, [⊗]Physics, [○]Chemistry, and [#]Veterinary & Biomedical Sciences, The Pennsylvania State University, University Park, Pennsylvania 16802, United States

Supporting Information

ABSTRACT: We present a configuration for fluorescence spectroscopy that exploits the optical properties of semitransparent gold films and widely available instrumentation. This method enables monitoring of biomolecule interactions with small molecules tethered on substrates in multicomponent environments. The neurotransmitter serotonin (5-hydroxytryptamine) was covalently attached to self-assembled monolayers on thin gold films at low density to facilitate antibody recognition. Protein-binding studies were performed in a fluorescently labeled immunoassay format. We find that the use of this method enables evaluation of nonspecific binding and relative quantification of specific binding between competing binding partners. This fluorescence spectroscopy technique has the potential to assess biosensor or medical device responses in complex biological matrices.

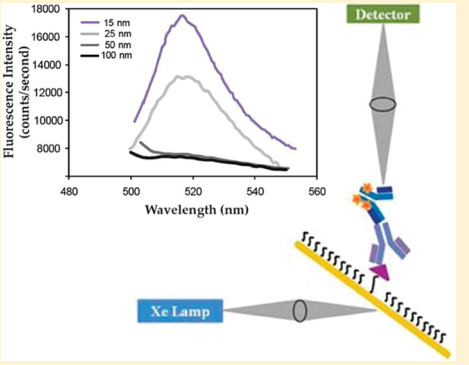

One of the key challenges in designing biocapture materials, such as those used in diagnostic devices and biosensors, is to enable specific and selective binding of analytes of interest in complex milieus.[1−5] Both label-free and label-based formats have been used to analyze interactions between surface-tethered probes and targets captured from solution. For instance, quartz crystal microgravimetry (QCM), a label-free technique that exploits the piezoelectric properties of quartz crystals, is used to measure changes in bound surface mass.[6−10] We have used QCM to investigate recognition and capture of antibodies and membrane-associated receptors by dilute surface-tethered small-molecule probes.[9,11,12] However, while label-free techniques offer simple sample preparation and analysis, the lack of chemically selective detection associated with these techniques remains a major challenge for sensing in real biological environments, e.g., plasma, serum, tissue, or culture media, which are composed of complex biomolecule mixtures.

Label-based methods provide an approach to the specific determination of binding partners. For example, surface-plasmon-enhanced fluorescence spectroscopy (SPFS) facilitates enhanced detection sensitivity, in combination with detection selectivity, using fluorescently tagged molecules.[13−15] The SPFS technique relies on the resonant excitation of surface plasmons at a metal−liquid interface to enhance the fluorescence signal of labeled biomolecules bound at the surface.[16] However, sophisticated optical instrumentation is necessary to produce surface plasmons and to measure fluorescence.

Here, we describe a novel method for sensing biomolecule binding to immobilized small-molecule partners using fluorescence spectroscopy. This technique does not require a custom-built optical configuration to excite fluorophores on gold surfaces. Instead, we exploit the optical properties of semitransparent continuous thin Au films[17] in our experimental design to excite surface-bound fluorescent labels. Binding is detected using a commercial fluorescence spectrometer. The neurotransmitter serotonin (5-hydroxytryptamine; 5-HT) was investigated as a prototypical small-molecule probe. Serotonin is an important signaling molecule in the central nervous system and periphery.[18−22] Serotonin was covalently tethered at low density to self-assembled monolayers (SAMs) that resist nonspecific binding interactions,[9,11,12] enabling selective detection of antibody binding partners (Figure 1).

Our goals are to develop a straightforward and accessible label-based immunoassay technique to distinguish and to quantify specific vs nonspecific binding and to assess relative binding between multiple biorecognition partners. While previous studies have focused on determining the binding of a single partner to a corresponding surface-tethered probe,[4,14,15] there has been substantially less work directed at understanding how multiple partners in competitive environments interact with tethered

Received: June 27, 2011
Accepted: August 25, 2011
Published: August 25, 2011

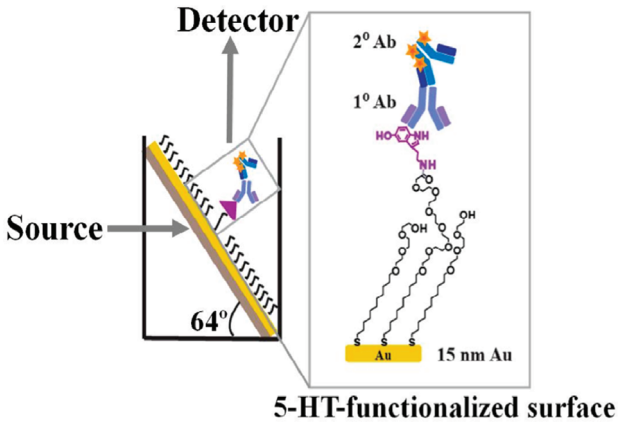

Figure 1. Schematic of antibody binding detected by fluorescence spectroscopy: Oligo(ethylene glycol)-terminated self-assembled monolayers on semitransparent 15-nm-thick Au films were functionalized at dilute coverage with serotonin (5-HT, purple triangle). Substrates were incubated with antiserotonin primary antibodies (1°Ab) and fluorescently labeled (orange ★) secondary antibodies (2°Ab), the latter of which recognize 1°Ab. Samples were placed in a water-filled cuvette at a 64° angle from the base of the cuvette.

probe systems. This type of study is important for determining the efficacy of probe-functionalized surfaces for capturing binding partners from mixtures containing single or multiple specific binding partner(s) in the presence of nonspecific proteins, where binding depends on the relative affinities of various targets for the probe. This represents a significant situation that requires optimization for sensing in complex biological environments.

MATERIALS AND METHODS

Chemicals. 23-(9-Mercaptononyl)-3,6,9,12,15,18,21-heptaoxatricosanoic acid and 1-(9-mercaptononyl)-3,6,9-trioxaundecan-11-ol were purchased from Toronto Research Chemicals (Toronto, ON). *N*-Ethyl-*N*-(dimethylaminopropyl)-carbodiimide (EDC), *N*-hydroxysuccinimide (NHS), 5-hydroxytryptamine hydrochloride (5-HT), fibrinogen, fibronectin, and bovine serum albumin (BSA) were obtained from Sigma-Aldrich (St. Louis, MO). Commercial grade ethanol (EtOH) was from Pharmaco-AAPER (Brookfield, CT). Antibodies (rabbit antiserotonin polyclonal and rat antiserotonin monoclonal) were procured from Millipore (Temecula, CA). Alexa Fluor 488-labeled goat antirabbit secondary antibody (excitation 495 nm, emission 518 nm) was purchased from Invitrogen (Carlsbad, CA). Substrates were prepared from custom cut 10 mm × 30 mm pieces of standard 1-mm-thick microscope glass slides (VWR International, West Chester, PA).

Thin Gold Films. Substrates were prepared by evaporating Au (15−100 nm) over a 1-nm Cr undercoat on 10 mm × 30 mm glass slides using an electron-beam evaporator (Kurt J. Lesker, Clairton, PA). Deposition was carried out at a rate of 1 Å/s. Substrates coated with Au were rinsed with deionized H_2O, followed by EtOH, then dried under a stream of N_2, and annealed using a H_2 flame for 1 min prior to monolayer formation.

Monolayer Preparation and Functionalization. Self-assembled monolayers were prepared by immersing Au substrates in a 1 mM solution of 1-(9-mercaptononyl)-3,6,9-trioxaundecan-11-ol. Carboxy-terminated tether molecules were then inserted into monolayer defects using a 0.2 mM solution of 23-(9-mercaptononyl)-3,6,9,12,15,18,21-heptaoxatricosanoic acid.[9,23−28] Terminal carboxyl groups in the resulting dilute mixed SAMs were ester activated to facilitate the formation of an amide bond between the serotonin primary amine and carboxyl groups on monolayer surfaces (Figure 1).[9]

Transmission UV−Visible Spectroscopy. Transmission spectra were obtained using a Lambda 950 UV−vis−NIR spectrophotometer (Perkin-Elmer, Waltham, MA). All measurements were carried out in a cuvette in air at room temperature. A plain glass sample was used to obtain measurements for baseline correction before each experimental measurement.

Atomic Force Microscopy. Images were acquired using a commercial Dimension 5000 atomic force microscope (Veeco Instruments, Santa Barbara, CA) in tapping mode. Images were obtained at a scan rate of 1 Hz using silicon cantilevers (Veeco Instruments, Santa Barbara, CA) and a scan size of 1 μm with a resonant frequency of 280 kHz.

Fluorescence Spectroscopy. Fluorescence emission spectra of surfaces were measured using a QM-4/2005 fluorescence spectrometer (Photon Technology International, Inc., Birmingham, NJ) equipped with a xenon lamp. This light source and detector were in the same plane at right angles to each other (Figure 1). Surfaces were maintained in a water-filled cuvette at a 64° angle from the base of the cuvette for fluorescence measurements, as shown in Figure 1. Samples were incubated with either rabbit antiserotonin polyclonal antibody (1:100 dilution from stock solution) or rabbit antiserotonin polyclonal antibody and varying ratios of rat antiserotonin monoclonal antibody (1:100 dilution from stock solution) for 45 min at room temperature. In other experiments, samples were incubated in a mixture of rabbit antiserotonin polyclonal antibody and the nonspecific proteins fibrinogen, fibronectin, or BSA for 45 min. For calculations of molar ratios, we used an antibody molecular mass of 150 kDa and a density of 2.4 mg/mL. Fibronectin, fibrinogen, and BSA molecular masses are 440, 340, and 66 kDa, respectively. All samples were exposed to Alexa Fluor 488-labeled goat antirabbit secondary antibody (1:200 dilution from stock solution) for 30 min, followed by rinsing for 10 s with deionized H_2O before fluorescence measurements. The secondary antibody is raised against rabbit IgG antibodies; thus, it selectively recognizes rabbit antiserotonin polyclonal antibodies vs rat antiserotonin monoclonal antibodies. Normalized fluorescence peak intensities were calculated by dividing the emission peak intensities collected from each sample after exposure to secondary antibodies by the emission peak intensities measured after exposure to primary antibodies alone.

RESULTS AND DISCUSSION

Transmission of Thin Gold Films. We characterized the transmission of light as a function of wavelength through substrates with Au films of varying thicknesses. Representative spectra, shown in Figure 2, illustrate that the transparency of the Au films decreases substantially with increasing thickness, as expected.[29−31] Maximum transmission decreased from 50% to 30% when the Au thickness was increased from 15 to 25 nm. Films with 15-nm-thick Au resulted in a transmission peak maximum (λ_{max}) at 521 nm, whereas 25-nm-thick Au films showed a blue-shifted λ_{max} at 515 nm.[31,32] For Au film thicknesses of 50 nm, transmission was negligible for the purpose of these experiments. We attribute the transmission peak at ~520 nm to electronic transitions and recombination between filled *d*-bands and the conduction band in the Au.[17,33] Atomic

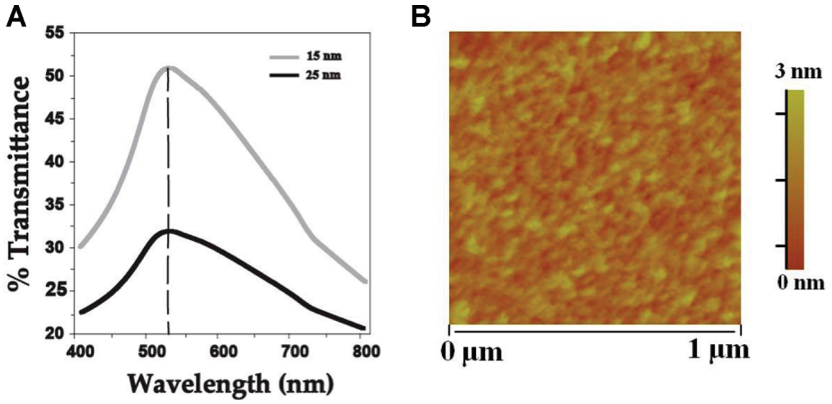

Figure 2. Effects of Au film thickness on transmission: Gold was deposited on glass substrates by controlled evaporation. Incident light was passed through the substrates. (A) Transmission was measured as a function of wavelength. The dotted line indicates the transmission maximum for 15-nm-thick Au substrates. (B) A representative topographic atomic force microscopy image of a 15-nm-thick continuous Au film on glass. Topographic features are indicative of the underlying glass surface roughness.

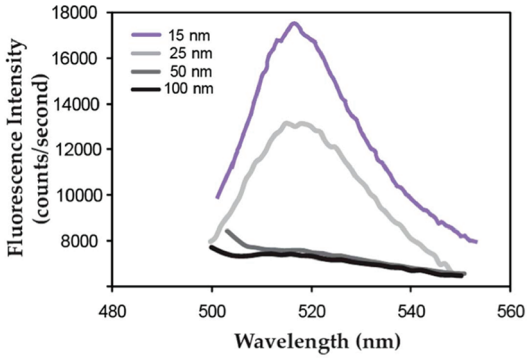

Figure 3. Fluorescence intensity associated with antibodies captured by bound serotonin depends on the Au film thickness. Fluorescence emission spectra were measured for antibodies captured by serotonin-functionalized self-assembled monolayers on varying thicknesses of Au on glass. Functionalized surfaces were incubated with primary antiserotonin antibodies followed by fluorescently tagged secondary antibodies (Alexa Fluor 488; peak emission 518 nm).

force microscopy analysis suggests that 15-nm-thick Au films on glass have continuous grain structure[31] with an average rms roughness of 2.1 nm (Figure 2).

Fluorescence Intensity of Serotonin Antibody Binding Depends on Au Thickness. We fabricated serotonin-functionalized SAMs[9,11,12] on Au films of varying thicknesses (15−100 nm). Substrates were incubated with primary antibodies that recognize tethered serotonin and fluorescently tagged secondary antibodies that bind to these primary antibodies. After antibody immobilization, the fluorophores on secondary antibodies are more than 10 nm from the Au surface, minimizing metal-induced quenching.[16,34,35] As shown in Figure 3, semitransparent Au layers less than 50 nm thick yield measurable fluorescence spectra, whereas the opaque, thicker Au layers produce no detectable emission spectra. Of the thicknesses tested, the emission peak was strongest for 15-nm-thick Au films, in agreement with the transmission data in Figure 2. We expect that because the skin depth of incident light of ∼500 nm wavelength is ∼20 nm for Au,[36] the lack of transmitted light for thicker Au substrates results in the absence of excitation of surface-bound fluorophores. Thus, 15-nm-thick Au films were used for further experiments. Others and we have observed that the monolayer quality on 15-nm-thick Au substrates is comparable to thicker Au substrates (>100 nm).[31]

In surface-plasmon-enhanced fluorescence spectroscopy, signals due to fluorescently tagged secondary antibody binding to primary antibodies captured on Au substrates are enhanced by surface plasmon resonance via the Kretchmann configuration.[14,16] With the use of this optical configuration, incident excitation light at the plasmon resonance angle is directed through a prism such that it impinges on an opaque Au layer grown on the back side of the prism where surface plasmons are excited. Fluorescence is measured via a photodetector positioned at the front (functionalized) side of the Au layer. For the fluorescence-spectroscopy-based design investigated here, incident light passes *through* a thin Au-film-coated substrate. The transparency of Au films on glass appears to be critical in this experimental configuration because substrates with Au film thicknesses that transmit measurable light (Figure 2) are integral to achieving fluorescence signals (Figure 3). Preliminary results indicated that the observed fluorescence emission is anisotropic (Figure S1 in the Supporting Information); emission intensity depends on sample orientation with respect to the incident light. The anisotropic nature of the fluorescence suggests that the emission signal might be affected by surface-mediated interactions.[37,38] The detailed mechanism of fluorescence emission associated with this type of Au surface using the optical configuration in Figure 1 is currently under investigation.

Serotonin-Functionalized Surfaces Resist Nonspecific Binding. Fibronectin, fibrinogen, and serum albumin are abundant components of extracellular and blood matrices and are commonly used to evaluate the fouling characteristics of surfaces.[5,39] As shown in Figure 4, no statistically significant changes in fluorescence intensity occurred when serotonin polyclonal antibodies were coincubated with the (unlabeled) nonspecific proteins fibronectin or fibrinogen (1:3 molar ratios) prior to exposing the samples to secondary antibodies. These results demonstrate that dilute functionalized substrates bearing oligo(ethylene glycol) largely prevent nonspecific binding in an environment where proteins simultaneously compete for binding epitopes.[4,5,9] Furthermore, specific binding is not inhibited by the presence of high concentrations of these nonspecific proteins.

Surfaces functionalized with serotonin showed a small amount of binding of bovine serum albumin (BSA) at high molar ratios

dx.doi.org/10.1021/ac2016536 |*Anal. Chem.* 2011, 83, 7451–7456

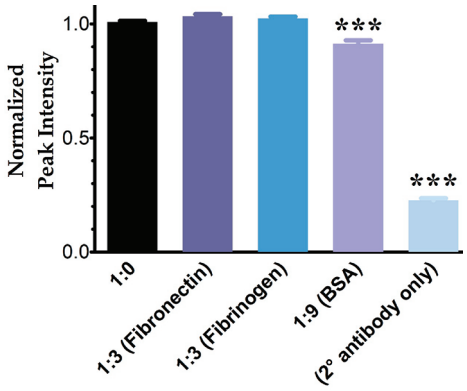

Figure 4. Serotonin-functionalized surfaces resist nonspecific protein adsorption: Ratios are molar concentrations of serotonin polyclonal antibody vs the nonspecific proteins fibronectin, fibrinogen, bovine serum albumin (BSA), and fluorescently tagged secondary antibodies (2° Ab). Error bars represent standard errors of the means for $N = 3$ samples per group. One-way analysis of variance indicated significant differences across means [$F(4,10)=1400$; $P < 0.001$]. Individual group comparisons were by Tukey's *post hoc* tests and are indicated by ***, $P < 0.001$ for 1:9 (BSA) or 2° antibody alone vs all other conditions.

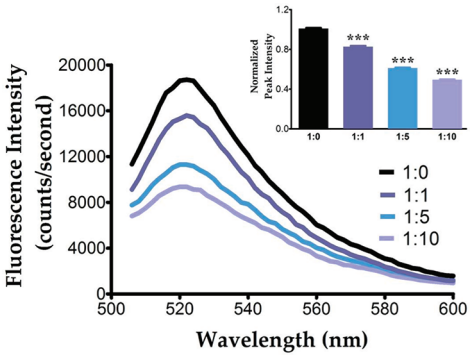

Figure 5. Competitive binding of different types of antibodies to surface-tethered serotonin by fluorescence spectroscopy: The ratios indicate the molar concentrations of serotonin polyclonal antibodies (pAb) vs serotonin monoclonal antibodies (mAb). Substrates were exposed to combinations of primary antibodies and subsequently incubated with fluorescently tagged secondary antibodies (Alexa Fluor 488; peak emission 518 nm), which recognize pAb but not mAb. The inset shows mean normalized peak intensities at various antibody ratios. Error bars represent standard errors of the means for $N = 3$ samples per group and are too small to visualize in some instances. One-way analysis of variance indicated a statistically significant difference across means [$F(3,8)=1300$; $P < 0.001$]. Individual group comparisons were evaluated by Tukey's *post hoc* tests and are indicated in the figure as ***, $P < 0.001$ for 1:1, 1:5, or 1:10 vs all other conditions.

(1:9), indicated by a 10% drop in peak fluorescence intensity (Figure 4). These data suggest that high concentrations of BSA slightly reduce the binding of the primary antibody to serotonin-functionalized surfaces or alternately, secondary antibody recognition of the primary antibody. We also investigated nonspecific binding using secondary antibodies alone. Secondary antibodies (2° Ab) were expected to lack specificity for surface-tethered serotonin. As shown in Figure 4, the normalized peak intensity for exposure to 2° Ab alone is only 20% of the binding of the combination of serotonin primary antibody plus fluorescently labeled secondary antibody. These results are consistent with previous results obtained using QCM measurements on serotonin-functionalized surfaces.[9,11]

Using QCM, we found that serotonin-functionalized surfaces specifically recognize serotonin antibodies compared to nonspecific IgG proteins and BSA; however, it was not possible to investigate nonspecific binding under competitive conditions. By employing the fluorescence-based method developed here, we demonstrate the selectivity of serotonin-functionalized surfaces for capturing binding partners from binary mixtures of a nonspecific protein (fibrinogen, fibronectin, or BSA) and a specific binding protein, serotonin polyclonal antibody. On the basis of these results, we hypothesize that binding detection of targets in complex environments, e.g., blood plasma or serum, will be possible using fluorescence spectroscopy provided that the SAM matrix resists nonspecific binding. While the oligo(ethylene glycol)-terminated SAMs used here enable discrimination between pairs of specific and nonspecific binding proteins, there is evidence that this type of SAM is not optimal for use with undiluted blood plasma or serum.[3] Future efforts will focus on developing zwitterionic polymers[40] or other types of oligo(ethylene glycol)-terminated thiols[41] capable of ultralow fouling for use with thin Au films, in combination with insertion strategies for dilute functionalization, to investigate biomolecule capture from complex biological matrices via fluorescence spectroscopy.

Even with the use of concentrations of antiserotonin polyclonal antibody as low as 15 nM, binding to serotonin-functionalized surfaces is detectable using the fluorescence-spectroscopy-based method described. In contrast, we were unable to detect binding responses of serotonin polyclonal antibodies at similar concentrations using QCM. While further studies to investigate the limits of detection by fluorescence spectroscopy are needed, this result, in conjunction with work by Knoll and co-workers,[16,42] suggest that limits of detection of label-based fluorescence spectroscopy methods are lower than label-free methods.

Detection of Multiple Binding Partner Interactions. Previously, we demonstrated via QCM that two different serotonin antibodies (one monoclonal and one polyclonal) recognize serotonin-functionalized surfaces.[9] However, as QCM is a label-free mass-based technique, it lacks the chemical selectivity needed to assess competitive interactions between high-affinity targets due to its inability to distinguish different bound species. By employing the fluorescence spectroscopy-based method developed here, we are able to investigate the relative capture of two different target proteins, both with specificity for the probe-functionalized surface. Serotonin-functionalized surfaces were challenged with serotonin polyclonal antibodies (pAb), in combination with increasing ratios of serotonin monoclonal antibodies (mAb), both of which compete for binding to surface-tethered serotonin. Subsequently, samples were exposed to fluorescently labeled antirabbit secondary antibodies, which selectively recognize rabbit pAb.

As shown in Figure 5, increasing relative concentrations of mAb results in lower fluorescence intensities. These data suggest that as the ratio of monoclonal antibodies increases, monoclonal antibodies outcompete polyclonal antibodies for specific binding sites. As a result, the number of fluorescently tagged secondary antibodies on the surface decreases because there are fewer surface-bound polyclonal antibodies.

We developed a quantitative model to determine the relative equilibrium affinity binding constants of competing binding partners in the type of three-component system used here.

We assume that serotonin polyclonal antibodies and serotonin monoclonal antibodies interact with surface-tethered serotonin such that the following equilibria exist:

$$5HT^* + pAb \xrightarrow{K_A^p} 5HT^*pAb \quad (1)$$

$$5HT^*pAb + 2Ab \overset{K_A^{p'}}{\rightleftharpoons} 5HT^*pAb2Ab \quad (2)$$

$$5HT^* + mAb \overset{K_A^m}{\rightleftharpoons} 5HT^*mAb \quad (3)$$

where pAb refers to serotonin polyclonal antibodies and mAb refers to serotonin monoclonal antibodies, both in solution, 5HT* refers to surface-tethered serotonin, and 5HT*pAb and 5HT*mAb are serotonin-bound polyclonal and monoclonal antibodies, respectively. Additionally, 5HT*pAb2Ab describes the surface-bound secondary antibody (2Ab)/polyclonal antibody complex. Secondary antibodies are assumed to recognize pAb vs mAb selectively. From these relationships, equilibrium-binding constants are given by

$$K_A^p = \frac{[5HT^*pAb]}{[5HT^*][pAb]} \quad (4)$$

$$K_A^p = \frac{[5HT^*pAb2pAb]}{[5HT^*][pAb]K_A^{p'}[2Ab]} \quad (5)$$

$$K_A^m = \frac{[5HT^*mAb]}{[5HT^*][mAb]} \quad (6)$$

where K_A^p and K_A^m are the equilibrium affinity constants for polyclonal and monoclonal antibodies, respectively. The equilibrium binding constant for eq 2 is substituted into eq 4 to get eq 5. In eq 5, $K_A^{p'}$ is defined as the equilibrium affinity constant for the interaction between secondary antibodies and surface-bound serotonin polyclonal antibodies. Here, $K_A^{p'}[2Ab] = 0.3$ based on an equilibrium binding constant of 0.003 nM^{-1} between surface-tethered rabbit antibody (IgG) and goat antirabbit IgG.[43] The concentration of goat antirabbit IgG ([2Ab]) in these experiments was ~100 nM.

K' is defined as the relative equilibrium affinity constant for polyclonal vs monoclonal antibodies and is obtained by dividing eq 5 by eq 6:

$$K' = \frac{K_A^p}{K_A^m} = \frac{[5HT^*pAb2Ab][mAb]}{0.3[5HT^*mAb][pAb]} \quad (7)$$

The normalized peak intensities from the inset in Figure 5 are proportional to polyclonal antibodies bound to serotonin-functionalized surfaces (5HT*pAb2Ab). Using the molar ratio of serotonin polyclonal (pAb) and monoclonal (mAb) antibodies in solution and the corresponding amounts of bound antibody, 5HT*pAb2Ab and 5HT*mAb, respectively, in eq 7, we calculate $K' = 23 \pm 5$. This result indicates that serotonin polyclonal antibodies have a 20-fold higher affinity for surface-tethered serotonin than monoclonal antibodies. We observed minimal cross reactivity (~2%) between antiserotonin monoclonal antibodies and the secondary antibody used in these experiments (Figure S2 in the Supporting information) indicating that changes in fluorescence intensities are directly related to changes in antiserotonin polyclonal primary antibody binding.

CONCLUSIONS AND PROSPECTS

We present a straightforward method that enables detection of biomolecule binding using semitransparent gold substrates and commercially available fluorescence spectrometers. Self-assembled monolayers functionalized at low density with the small-molecule neurotransmitter serotonin were used to study antibody recognition under competitive conditions to investigate binding specificity and selectivity. Our findings show that these surfaces are capable of selectively capturing specific binding partners from mixtures containing common plasma and extracellular matrix proteins found in high abundance in biological tissues. The use of the fluorescence spectroscopy method described here enables investigation of competitive binding behavior between targets with similar specificities, indicating that small-molecule-functionalized surfaces are capable of capturing multiple proteins from complex mixtures based on their affinities for surface-bound targets and relative concentrations. Comparative interaction strengths of binding partners were calculated without *a priori* knowledge of the absolute binding affinities.

We believe this fluorescence spectroscopy method will prove applicable to the study of a wide range of bimolecular interactions on surfaces, including receptor−ligand and nucleic acid systems. For example, in place of QCM,[11] receptors captured on small-molecule-functionalized surfaces might be detected using fluorescently tagged antireceptor antibodies via fluorescent spectroscopy on thin gold films. This technique could also be employed to monitor DNA hybridization using fluorescently tagged target strand binding to surface-immobilized complementary single-stranded DNA probes.[44] The success of fluorescence spectroscopy to study biochemical interactions depends on the use of semitransparent gold substrates and on capturing fluorophores above the critical distance (10 nm) from the gold substrate to circumvent fluorescence quenching.[45] Moreover, this technique, as currently configured, is most efficient for fluorophores with excitation wavelengths between 500 and 540 nm because of the higher transparency of thin Au films in this range. However, we envision that by incorporating Au-nanomaterial-based localized SPR, fluorescence spectroscopy can be applied throughout the visible spectrum for the detection of multiple fluorophores.[46−51]

ASSOCIATED CONTENT

Supporting Information. Additional information is available on the orientation dependence of fluorescence measurements and secondary antibody binding to serotonin-functionalized substrates. This material is available free of charge via the Internet at http://pubs.acs.org.

AUTHOR INFORMATION

Corresponding Author

*Anne Milasincic Andrews: address, Neuroscience Research Building, MC 957332, 635 Charles E. Young Dr. South, University of California, Los Angeles, Los Angeles, CA 90095-7332; phone, (310) 794-9421; e-mail, aandrews@mednet.ucla.edu. Paul S. Weiss: address, California NanoSystems Institute, 570 Westwood Plaza, Bldg. 114, MC 722710, University of California, Los Angeles, Los Angeles, CA 90095-7227; phone, (310) 267-5993; e-mail, psw@cnsi.ucla.edu.

■ ACKNOWLEDGMENT

The authors gratefully acknowledge Dr. Yogesh Singh and Ms. Stefanie Altieri for assistance with the graphics and Dr. Yuebing Zheng for insightful discussions. Prof. Michael Pishko is acknowledged with regard to the fluorescence spectroscopy experiments. The National Science Foundation, the Pennsylvania State University Huck Institutes of the Life Sciences, and the Kavli Foundation are acknowledged for financial support.

■ REFERENCES

(1) Rosi, N. L.; Mirkin, C. A. *Chem. Rev.* **2005**, *105*, 1547–1562.
(2) Senaratne, W.; Andruzzi, L.; Ober, C. K. *Biomacromolecules* **2005**, *6*, 2427–2448.
(3) Jiang, S.; Cao, Z. *Adv. Mater.* **2010**, *22*, 920–932.
(4) Mrksich, M.; Grunwell, J. R.; Whitesides, G. M. *J. Am. Chem. Soc.* **1995**, *117*, 12009–12010.
(5) Lahiri, J.; Isaacs, L.; Tien, J.; Whitesides, G. M. *Anal. Chem.* **1999**, *71*, 777–790.
(6) Rickert, J.; Brecht, A.; Göpel, W. *Biosens. Bioelectron.* **1997**, *12*, 567–575.
(7) Cans, A. S.; Höök, F.; Shupliakov, O.; Ewing, A. G.; Eriksson, P. S.; Brodin, L.; Orwar, O. *Anal. Chem.* **2001**, *73*, 5805–5811.
(8) Höök, F.; Kasemo, B.; Nylander, T.; Fant, C.; Sott, K.; Elwing, H. *Anal. Chem.* **2001**, *73*, 5796–5804.
(9) Shuster, M. J.; Vaish, A.; Szapacs, M. E.; Anderson, M. E.; Weiss, P. S.; Andrews, A. M. *Adv. Mater.* **2008**, *20*, 164–167.
(10) Wang, T.; Muthuswamy, J. *Anal. Chem.* **2008**, *80*, 8576–8582.
(11) Vaish, A.; Shuster, M. J.; Cheunkar, S.; Singh, Y. S.; Weiss, P. S.; Andrews, A. M. *ACS Chem. Neurosci.* **2010**, *1*, 495–504.
(12) Vaish, A.; Shuster, M. J.; Cheunkar, S.; Weiss, P. S.; Andrews, A. M. *Small* **2011**, *7*, 1471–1479.
(13) Roy, S.; Kim, J.-H.; Kellis, J. T.; Poulose, A. J.; Robertson, C. R.; Gast, A. P. *Langmuir* **2002**, *18*, 6319–6323.
(14) Yu, F.; Yao, D.; Knoll, W. *Anal. Chem.* **2003**, *75*, 2610–2617.
(15) Yu, F.; Persson, B.; Löfås, S.; Knoll, W. *Anal. Chem.* **2004**, *76*, 6765–6770.
(16) Liebermann, T.; Knoll, W. *Colloids Surf., A: Physicochem. Eng. Asp.* **2000**, *171*, 115–130.
(17) Mooradian, A. *Phys. Rev. Lett.* **1969**, *22*, 185.
(18) Murphy, D. L.; Fox, M. A.; Timpano, K. R.; Moya, P. R.; Ren-Patterson, R.; Andrews, A. M.; Holmes, A.; Lesch, K. P.; Wendland, J. R. *Neuropharmacology* **2008**, *55*, 932–960.
(19) Singh, Y. S.; Sawarynski, L. E.; Michael, H. M.; Ferrell, R. E.; Murphey-Corb, M. A.; Swain, G. M.; Patel, B. A.; Andrews, A. M. *ACS Chem. Neurosci.* **2010**, *1*, 49–64.
(20) Zhu, C. B.; Lindler, K. M.; Owens, A. W.; Daws, L. C.; Blakely, R. D.; Hewlett, W. A. *Neuropsychopharmacology* **2010**, *35*, 2510–2520.
(21) Ge, S.; Woo, E.; White, J. G.; Haynes, C. L. *Anal. Chem.* **2011**, *83*, 2598–2604.
(22) Singh, Y. S.; Altieri, S. C.; Sibille, E.; Andrews, A. M. In *Neurobiology of Depression*; López-Muñoz, F., Álamo, C., Eds.; Taylor and Francis Group, LLC: Boca Raton, FL, in press.
(23) Donhauser, Z. J.; Mantooth, B. A.; Kelly, K. F.; Bumm, L. A.; Monnell, J. D.; Stapleton, J. J.; Price, D. W., Jr.; Rawlett, A. M.; Allara, D. L.; Tour, J. M.; Weiss, P. S. *Science* **2001**, *292*, 2303–2307.
(24) Lewis, P. A.; Donhauser, Z. J.; Mantooth, B. A.; Smith, R. K.; Bumm, L. A.; Kelly, K. F.; Weiss, P. S. *Nanotechnology* **2001**, *12*, 231–237.
(25) Lewis, P. A.; Inman, C. E.; Yao, Y.; Tour, J. M.; Hutchison, J. E.; Weiss, P. S. *J. Am. Chem. Soc.* **2004**, *126*, 12214–12215.
(26) Mullen, T. J.; Dameron, A. A.; Andrews, A. M.; Weiss, P. S. *Aldrichim. Acta* **2007**, *40*, 21–31.
(27) Mullen, T. J.; Srinivasan, C.; Shuster, M. J.; Horn, M. W.; Andrews, A. M.; Weiss, P. S. *J. Nanopart. Res.* **2008**, *10*, 1231–1240.
(28) Kim, M.; Hohman, J. N.; Cao, Y.; Houk, K. N.; Ma, H.; Jen, A. K.; Weiss, P. S. *Science* **2011**, *331*, 1312–1315.
(29) DiMilla, P. A.; Folkers, J. P.; Biebuyck, H. A.; Haerter, R.; Lopez, G. P.; Whitesides, G. M. *J. Am. Chem. Soc.* **1994**, *116*, 2225–2226.
(30) Doron-Mor, I.; Barkay, Z.; Filip-Granit, N.; Vaskevich, A.; Rubinstein, I. *Chem. Mater.* **2004**, *16*, 3476–3483.
(31) Wanunu, M.; Vaskevich, A.; Rubinstein, I. *J. Am. Chem. Soc.* **2004**, *126*, 5569–5576.
(32) Khriachtchev, L.; Heikkila, L.; Kuusela, T. *Appl. Phys. Lett.* **2001**, *78*, 1994–1996.
(33) Ahn, W.; Taylor, B.; Dall'Asen, A. G.; Roper, D. K. *Langmuir* **2008**, *24*, 4174–4184.
(34) Adamson, A. W.; Gast, A. P. *Physical Chemistry of Surfaces*, 6th ed.; Wiley Interscience: New York, 1997.
(35) Lakowicz, J.; Geddes, C.; Gryczynski, I.; Malicka, J.; Gryczynski, Z.; Aslan, K.; Lukomska, J.; Matveeva, E.; Zhang, J.; Badugu, R.; Huang, J. *J. Fluoresc.* **2004**, *14*, 425–441.
(36) Scalora, M.; Bloemer, M. J.; Pethel, A. S.; Dowling, J. P.; Bowden, C. M.; Manka, A. S. *J. Appl. Phys.* **1998**, *83*, 2377–2383.
(37) Weber, W. H.; Eagen, C. F. *Opt. Lett.* **1979**, *4*, 236–238.
(38) Matveeva, E. G.; Gryczynski, Z.; Malicka, J.; Lukomska, J.; Makowiec, S.; Berndt, K. W.; Lakowicz, J. R.; Gryczynski, I. *Anal. Biochem.* **2005**, *344*, 161–167.
(39) Chang, Y.; Chen, S.; Zhang, Z.; Jiang, S. *Langmuir* **2006**, *22*, 2222–2226.
(40) Vaisocherova, H.; Yang, W.; Zhang, Z.; Cao, Z.; Cheng, G.; Piliarik, M.; Homola, J.; Jiang, S. *Anal. Chem.* **2008**, *80*, 7894–7901.
(41) Vanderah, D. J.; Vierling, R. J.; Walker, M. L. *Langmuir* **2009**, *25*, 5026–5030.
(42) Yu, F.; Yao, D.; Knoll, W. *Anal. Chem.* **2003**, *75*, 2610–2617.
(43) Gish, D. A.; Nsiah, F.; McDermott, M. T.; Brett, M. J. *Anal. Chem.* **2007**, *79*, 4228–4232.
(44) Gillmor, S. D.; Thiel, A. J.; Strother, T. C.; Smith, L. M.; Lagally, M. G. *Langmuir* **2000**, *16*, 7223–7228.
(45) Lakowicz, J. R. *Anal. Biochem.* **2001**, *298*, 1–24.
(46) Haes, A. J.; Van Duyne, R. P. *J. Am. Chem. Soc.* **2002**, *124*, 10596–10604.
(47) Rosenthal, S. J.; Tomlinson, I.; Adkins, E. M.; Schroeter, S.; Adams, S.; Swafford, L.; McBride, J.; Wang, Y.; DeFelice, L. J.; Blakely, R. D. *J. Am. Chem. Soc.* **2002**, *124*, 4586–4594.
(48) Haes, A. J.; Van Duyne, R. P. *Anal. Bioanal. Chem.* **2004**, *379*, 920–930.
(49) Lahav, M.; Vaskevich, A.; Rubinstein, I. *Langmuir* **2004**, *20*, 7365–7367.
(50) Liao, W.-S.; Chen, X.; Yang, T.; Castellana, E. T.; Chen, J.; Cremer, P. S. *Biointerphases* **2009**, *4*, 80–85.
(51) Wittenberg, N. J.; Haynes, C. L. *Wiley Interdiscip. Rev. Nanomed. Nanobiotechnol.* **2009**, *1*, 237–254.